

**$\gamma\gamma$  angular-correlation analysis of  $^{200}\text{Hg}$  after cold-neutron capture**C. Bernards,<sup>1,2,\*</sup> W. Urban,<sup>3,4</sup> M. Jentschel,<sup>4</sup> B. Märkisch,<sup>4,†</sup> J. Jolie,<sup>1</sup> C. Fransen,<sup>1</sup> U. Köster,<sup>4</sup> T. Materna,<sup>4,‡</sup> G. S. Simpson,<sup>5</sup> and T. Thomas<sup>1</sup><sup>1</sup>*Institut für Kernphysik, Universität zu Köln, Zùlpicher Straße 77, D-50937 Köln, Germany*<sup>2</sup>*Wright Nuclear Structure Laboratory, Yale University, New Haven, Connecticut 06520, USA*<sup>3</sup>*Faculty of Physics, University of Warsaw, ul. Hoza 69, PL-00-681 Warsaw, Poland*<sup>4</sup>*Institut Laue-Langevin, 6 rue J. Horowitz, F-38042 Grenoble, France*<sup>5</sup>*LPSC, Université Joseph Fourier Grenoble 1, CNRS/IN2P3, Institut National Polytechnique de Grenoble, F-38026 Grenoble Cedex, France*

(Received 31 July 2011; revised manuscript received 12 October 2011; published 31 October 2011;

publisher error corrected 2 November 2011)

We report on a  $\gamma\gamma$  angular-correlation experiment investigating  $^{200}\text{Hg}$  after cold-neutron capture. The experiment was performed using eight high-purity germanium detectors mounted on an array installed at the PFIB neutron beam line of the research reactor of the Institut Laue-Langevin in Grenoble, France. The geometry of the array allows  $\gamma\gamma$  angular-correlation analyses that can be used for the determination of level spins and multipole mixing ratios in  $^{200}\text{Hg}$ . We present multipole mixing ratios for secondary  $\gamma$  rays and investigate the nature of the  $^{200}\text{Hg}$  neutron-capture state by analyzing the observed primary  $\gamma$  rays of this nucleus.

DOI: [10.1103/PhysRevC.84.047304](https://doi.org/10.1103/PhysRevC.84.047304)

PACS number(s): 23.20.En, 23.20.Gq, 27.80.+w, 28.20.Np

The investigation of neutron-capture reactions allows a rather complete spectroscopy of excited low-spin nuclear states [1]. Because there is no Coulomb interaction for neutrons, the cold neutrons ( $E_n \approx 4\text{--}5$  meV) available at the PFIB beam line [2,3] of the research reactor of the Institut Laue-Langevin (ILL) can populate capture states in nuclei with the excitation energy  $E_x = S_n + E_n \approx S_n$ . The neutron-separation energy,  $S_n$ , is 8028.40 keV for  $^{200}\text{Hg}$  [4]. The  $\gamma$ -decay spectrum following neutron capture consists of two components: primary and secondary  $\gamma$  rays, respectively. Their observation and analysis give insights into the underlying structure of the nucleus. The radiation of the high-energy primary  $\gamma$  rays, directly populating states from the neutron-capture state, is usually of  $E1$  character, whereas the multipolarity of the rather low-energy secondary  $\gamma$  rays cannot be predicted easily. In general, the multipolarity of  $\gamma$  transitions depends on the initial- and final-level spin and parity and the energy of the  $\gamma$  transition itself.

For the cold neutron-capture reaction  $^{199}\text{Hg}(n, \gamma)^{200}\text{Hg}$ , there are two spin possibilities for the capture state in  $^{200}\text{Hg}$ . Its spin depends on the ground-state spin  $I = 1/2^-$  of  $^{199}\text{Hg}$  [5], the angular momentum of the captured neutron, which is for cold neutrons  $\ell = 0$ , and the spin  $s = 1/2$  of the captured neutron. The possible spin and parity of the capture state follow the relations  $I' = I + \ell + s$  and  $\pi' = (-1)^\ell \pi$  [1], resulting in  $I' = 0^-$  or  $I' = 1^-$  for  $^{200}\text{Hg}$ . Since the lowest-lying neutron-capture resonance is at 33.5(1) eV and has a width of  $\Gamma \ll 1$  eV [6] far away from the maximum energy of cold neutrons, one can expect to not get into a resonance while populating  $^{200}\text{Hg}$  with cold neutrons. Therefore, we

only populate the neutron-capture state, being of spin  $0^-$  or  $1^-$ . Given the fact that the most likely radiation character for the primary  $\gamma$  rays is  $E1$ , the vast majority of primary  $\gamma$  rays should change parity and fulfill the  $\Delta J = 0$  or 1 condition. It is important to note that the spin of the neutron-capture state is not necessarily unambiguous. Neglecting a spin contribution, e.g., when investigating primary  $\gamma$  rays, might cause conflicting results, since the measured primary  $\gamma$  rays might be a mixture originating from both possible capture states.

Populating the  $^{200}\text{Hg}$  isotope via neutron capture is rather easy, as it is possible to use natural mercury as a target material. The neutron-capture cross section for the reaction  $^{199}\text{Hg}(n, \gamma)$  is  $\sigma_{\text{th}} \approx 2100$  b for thermal neutrons, which is more than 99.9% of the total  $^{\text{nat}}\text{Hg}$  neutron-capture cross section. To populate excited states in  $^{200}\text{Hg}$ , we irradiated a target (diameter  $< 5$  mm) consisting of 7 mg of natural HgS, sealed in a Teflon bag, with cold neutrons. For this measurement we have used two days of beam time. The  $(n, \gamma\gamma)$  angular-correlation array we have used consists of eight high-purity germanium detectors, mounted in a plane perpendicular to the neutron beam line in octahedral geometry ( $45^\circ$  steps). The distance between the target and the front surface of the germanium detectors was 12 cm. To avoid damaging the detectors and to minimize the background due to unwanted other reactions induced by neutrons (or scattered neutrons), we applied a combined shielding of boron, lithium, and lead around the beam line, on both sides of the array. The beam diameter after the collimator was 1 cm with an estimated neutron flux of  $5 \times 10^7 \text{ s}^{-1} \text{ cm}^{-2}$ . The acquired data of the detectors were processed and saved in list mode using digital XIA electronics with a 40-MHz clock [7]. We performed the energy and efficiency calibration using the well-known energies and intensities of a  $^{152}\text{Eu}$  calibration source for the low-energy part and  $\gamma$  rays following the neutron capture by a  $^{35}\text{Cl}$  target to calibrate up to the neutron-separation energy of  $^{200}\text{Hg}$ .

The geometry of the setup allows the measurement of  $\gamma\gamma$  angular correlations. Such correlations can be used to

\*bernards@ikp.uni-koeln.de

<sup>†</sup>Present address: Physikalisches Institut, Universität Heidelberg, Philosophenweg 12, D-69120 Heidelberg, Germany.<sup>‡</sup>Present address: CEA, DSM-Saclay, IRFU/SPhN, F-91191 Gif-sur-Yvette, France.

determine level spins and multipole mixing ratios  $\delta$  of  $\gamma$  transitions in a cascade, linking three levels with spin  $J_1$ ,  $J_2$ , and  $J_3$  as follows:  $J_1 \xrightarrow{\gamma_1, \delta_1} J_2 \xrightarrow{\gamma_2, \delta_2} J_3$ . For the analysis, pairs of  $\gamma$  signals detected in time coincidence were sorted into three different matrices, depending on the angles between the associated detector pairs, i.e., the relative angles  $\phi$  between the detector axes. There are three of these ‘‘correlation groups’’: 1:  $\phi = 45^\circ$  or  $135^\circ$  (32 detector pairs), 2:  $90^\circ$  or  $270^\circ$  (16 pairs), and 3:  $180^\circ$  (8 pairs). We have used this technique also in Refs. [8,9]. The theory we used to analyze the measured angular distribution is described in Refs. [10–12]. Based on the geometry of the setup we determined attenuation factors to account for the finite detector sizes. We have used a modified version of the computer code CORLEONE [13,14] to analyze the  $\gamma\gamma$  angular correlations. To determine spins and mixing coefficients, we fitted theoretical  $\gamma\gamma$  angular correlations to the measured  $\gamma$  intensities in different correlation groups, comparing various spin hypotheses and fitting the multipole mixing ratio.

Table I lists the results of our angular-correlation analysis. In total, we could determine multipole mixing ratios for 16

different  $\gamma$  transitions. It is interesting to note that some of our multipole mixing ratios differ significantly from the ones given in Ref. [4]. For other transitions the absolute  $\delta$  values are in agreement but have a different sign. The phase convention we use, and therewith the sign of our multipole mixing ratio  $\delta$ , follows the Krane and Steffen convention [10,11]. The usage of the Rose-Brink convention [15] for previously published values could explain differing signs. The published data [4] on  $\delta$  values originate mainly from experiments investigating  $^{200}\text{Hg}$  after  $\beta$  decay of a  $^{200}\text{Tl}$  source and from neutron-capture measurements [16–19]. Some of these  $\delta$  values have been obtained using the  $\gamma\gamma$  correlation analysis technique. Unfortunately, we could not clarify which phase convention was used for the published multipole mixing ratios.

In the analysis of the  $\gamma\gamma$  coincidences we found the 1225-keV line to be a doublet, which has not been reported in previous experiments. For the analysis of the  $\gamma\gamma$  angular correlations this information has to be taken into account. We can place the  $\gamma$ -ray transition of 1225.1 keV between the 3569-keV ( $1^+$ ) and the 2344-keV ( $3^+$ ) levels,

TABLE I. Comparison of our determined multipole mixing ratios  $\delta$  and data taken from the literature [4]. All listed  $\delta$  values were determined by angular correlations between secondary  $\gamma$  rays. The listed  $\gamma$  multiplicities refer to our  $\delta$  values. In addition, we give primary  $\gamma$ -ray energies  $E_\gamma^{\text{prim}}$  with their associated levels up to a level energy of 3 MeV. Due to the level density, the primary  $\gamma$ -ray energies were determined in coincidence spectra; therefore the errors are quite large in case of poor statistics. The sign convention we use for the multipole mixing ratio  $\delta$  follows the Krane and Steffen convention [10,11].

$E_{\text{Level}}$ (keV)	$J^\pi$ (Ref. [4])	$E_\gamma^{\text{prim}}$ (keV)	$E_\gamma^{\text{sec}}$ (keV)	$\delta$ (this work)	$\delta$ (Ref. [4])	$\gamma$ multipolarity	$E_{\text{Final}}$ (keV)	$J_{\text{Final}}^\pi$
368	$2^+$	7659.06						
947	$4^+$		578.92	$-0.02(3)$		$E2$	368	$2^+$
1029	$0^+$	6999.48						
1254	$2^+$	6772.56	885.82	$-1.72(12)$	$-2.20_{-5}^{+16}$	$E2(+M1)$	368	$2^+$
1570	$1^+$	6457.46	1202.02	$-0.43(4)$	$+0.16(5)$	$E2 + M1$	368	$2^+$
1574	$2^+$	6454.48	1205.42	$+0.26(2)$	$-0.25_{-2}^{+3}$	$E2 + M1$	368	$2^+$
1593	$2^+$	6434.86	1225.43	$-0.09(15)$	$-2.5_{-3}^{+2}$	$M1(+E2)$	368	$2^+$
1631	$1^+$	6396.86	1262.72	$+0.12(5)$	$+0.5(3)$	$M1 + E2$	368	$2^+$
1641	$2^+$	6388.010	1273.22	$+0.02(3)$	$+0.05(3)$	$M1(+E2)$	368	$2^+$
1718	$1^+$	6309.56	1350.12	$+0.03(5)$	$-0.036(24)$	$M1(+E2)$	368	$2^+$
1731	$2^+$	6296.310	783.32	$-0.04(6)$		$E2$	947	$4^+$
			1362.82	$-0.38(15)$	$-1.0_{-5}^{+2}$	$E2 + M1$	368	$2^+$
1734	$3^+$		786.82	$+0.08(4)$		$M1 + E2$	947	$4^+$
1776	$3^+$		828.02	$-0.04(3)$	$-0.04(5)$	$M1(+E2)$	947	$4^+$
1846	$3^+$		898.22	$-0.07(4)$	$\approx 0.5$	$M1 + E2$	947	$4^+$
1883	$2^+$		1514.52	$+0.10(4)$	$-0.14(4)$	$M1 + E2$	368	$2^+$
1972	$2^+$		1604.22	$+0.15(4)$	$+0.87(18)$	$M1 + E2$	368	$2^+$
2061	$1^+$	5966.64	1692.92	$-0.03(2)$	$+0.003(13)$	$M1(+E2)$	368	$2^+$
2189	$1^+$	5842.015						
2229	$1^+$	5799.06	974.82		$\approx 0.8$		1254	$2^+$
2274	$(1, 2)^+$	5753.715						
2289	$2^+$	5740.28						
2296	$1^+$	5731.84						
2344	$(3)^+$	5684.215						
2370	$1^+$	5658.14	2001.72		$-0.014(19)$		368	$2^+$
2462	$1^{(+)}$	5566.85						
2640	$1^+$	5388.54						
2692	$(1, 2)^+$	5336.310						
2878	$1^+$	5149.95						
2978	$1^+$	5049.94						

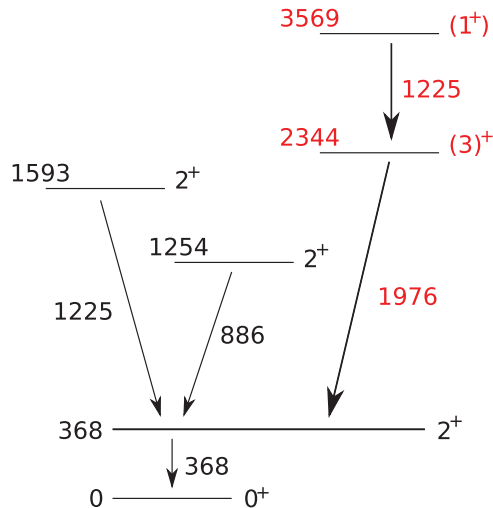


FIG. 1. (Color online) Partial level scheme of  $^{200}\text{Hg}$  used for the discussion of the multipolarity of the 1225.4-keV transition depopulating the 1593-keV level. The red branch on the right-hand side shows the newly placed, second component of the 1225-keV doublet.  $\gamma$  transition and level energies are given in keV.

as shown in the partial level scheme in Fig. 1. This second 1225-keV transition is also in coincidence with the 367.7-keV ground-state transition. Therefore, its influence on  $\gamma\gamma$  angular correlations has to be taken into account when analyzing the  $1593 \rightarrow 368 \rightarrow 0$  keV cascade. The resulting angular correlations give a value of  $\delta = -0.09(15)$  for the 1225.4-keV  $\gamma$ -ray transition between the 1593- and 368-keV levels. This value has a relatively large error due to the more complex analysis. Figure 2(a) shows a  $\tan^{-1}\delta$  plot of the 1225.4-keV transition, visualizing the deviation between the measured angular distribution and the calculated distribution for different spin hypotheses while varying  $\delta$ . The spin hypothesis of  $J_1 = 2$  describes the measured distribution best and shows an unambiguous minimum in agreement with  $\delta = -0.09(15)$ .

Our result clearly differs from the value  $\delta = -2.5_{-3}^{+2}$  for the 1225.4-keV transition depopulating the 1593-keV level reported in Ref. [19]. It is uncertain where that difference comes from. Even if we ignore our information on the 1225-keV doublet and do not correct for it, we still measure a small multipole mixing ratio for that transition of  $-0.1 < \delta < 0$ . Therefore, we tested the sensitivity of our  $\gamma\gamma$  angular-correlation setup: we note that the value of  $\delta = -2.5_{-3}^{+2}$  [19] is comparable to  $\delta = -1.72(12)$  determined in our work for the 885.8-keV transition depopulating the  $2_2^+$  state. Both the 885.8-keV and the 1225.4-keV transition are in cascades with the same spin sequence  $2 \rightarrow 2 \rightarrow 0$ . Therefore, considering similar  $\delta$  values and the common  $\gamma_2 = 367.7$ -keV transition, one expects similar  $\tan^{-1}\delta$  plots for both cascades. Indeed, the  $\tan^{-1}\delta$  plot shown in Fig. 2 of Ref. [19]—assuming the 1574 keV in the caption should read 1593 keV—for their analysis of the 1225.4-keV transition looks very similar to the  $\tan^{-1}\delta$  plot for the 885.8-keV transition obtained in this work, shown in Fig. 2(b). This shows that the sensitivity of both setups seems to be comparable and does not explain the discrepancy of the  $\delta$  values for the 1593- to 368-keV transition.

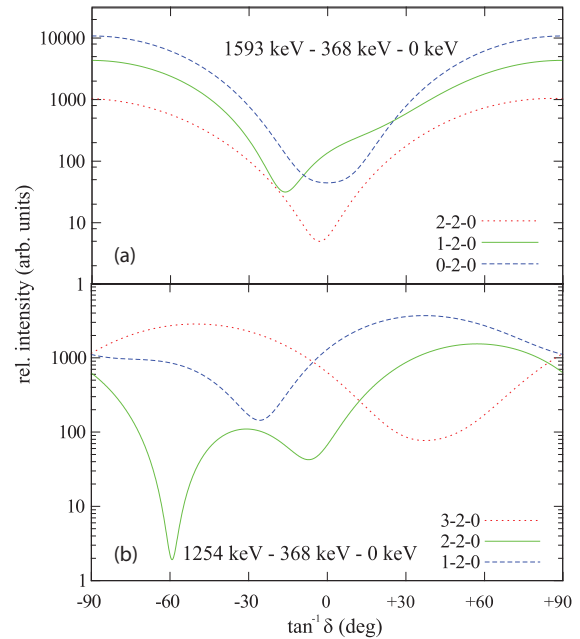


FIG. 2. (Color online) (a) A  $\tan^{-1}\delta$  plot for the  $\gamma$ -ray cascade  $1593 \rightarrow 368 \rightarrow 0$  keV. We compare an initial state of spin  $J_1 = 2, 1, 0$  with our data by varying the multipole mixing ratio  $\delta$  of the 1225.4-keV transition from  $\delta_1 = \tan(-90^\circ)$  to  $\tan(+90^\circ)$ . The data support the spin  $J_1 = 2$  assignment and are in agreement with  $\delta_1 = -0.09(15)$ . (b) A  $\tan^{-1}\delta$  plot for the  $1254 \rightarrow 368 \rightarrow 0$  keV  $\gamma$ -ray cascade. The global minimum for the spin  $J_1 = 2$  assumption is in agreement with  $\delta_1 = -1.72(12)$  and is similar to the published multipole mixing ratio for the 1225.4-keV  $1593 \rightarrow 368$  keV transition in Ref. [19]. The  $\tan^{-1}\delta$  plot in this figure looks similar to the one shown in Fig. 2 of Ref. [19].

In the literature, the neutron-capture state in  $^{200}\text{Hg}$  is assumed to be dominated by a  $0^-$  state [20,21]. However, the direct population of  $2^+$  states in  $^{200}\text{Hg}$  following cold-neutron capture (see Table I), together with the primary  $\gamma$ -ray transition to the  $0^+$  state at 1029 keV, shows that there is a spin  $1^-$  contribution to the neutron-capture state in  $^{200}\text{Hg}$ . As we do not use a method populating all existing capture resonances, such as the so-called average resonance capture (ARC) process, it is possible that the  $0^-$  and  $1^-$  capture states do not give the same contribution to our data [22]. Indeed, this is also reflected in our results. Although there are plenty of  $2^+$  states being populated by primary  $\gamma$  rays, our data are not conflicting with the assumption of a dominating  $0^-$  capture state. The most intensive primary  $\gamma$  rays are the ones that are populating  $1^+$  states. This cannot confirm the neutron-capture state to be dominated by spin  $0^-$ , as the selection rules allow spin  $1^+$  states being populated by both possible capture states,  $0^-$  or  $1^-$ , via an  $E1$  transition. In case of an ARC process, we would expect the levels with spin  $0^+, 1^+$ , and  $2^+$  to be populated via primary  $\gamma$  rays—in a simple approximation—following the ratio 1:2:1 [22]. We can only show that there are certainly different contributions to the neutron-capture state: in the single spectra we observe a broad peak at 8024.1 keV. Its width of 12 keV is slightly larger than other peaks ( $\sim 9$  keV) in that energy region; therefore it may contain the 8028.4-keV

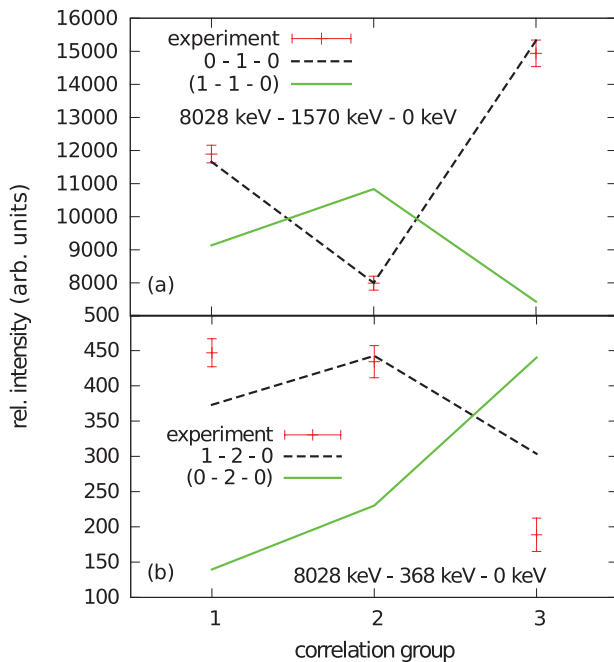


FIG. 3. (Color online) (a) Angular-correlation plot of a cascade including a primary  $\gamma$ -ray transition  $8028 \rightarrow 1570 \rightarrow 0$  keV. We compare an initial state of spin  $J_1 = 0$  with one having  $J_1 = 1$ . Our experimental values are in very good agreement with the  $J_1 = 0$  assumption. (b) Comparison between a hypothetical  $M2$  primary  $\gamma$ -ray transition in the  $0^- \rightarrow 2^+ \rightarrow 0^+$  cascade and the  $1^- \rightarrow 2^+ \rightarrow 0^+$  cascade assuming an  $E1$  primary  $\gamma$  ray. Our data favor the  $J_1 = 1$  hypothesis.

transition from the neutron-capture state to the ground state of the nucleus. This  $\gamma$  transition could only originate from the  $1^-$  contribution of the capture state, as it would otherwise correspond to an  $E0$   $\gamma$ -ray transition. Another possibility to show the different spin contributions of the capture state is to

use angular-correlation plots. In Fig. 3(a) we plot the angular correlation of the 6457.4-keV primary  $\gamma$  and the 1569.8-keV secondary  $\gamma$  transition. We fixed both transitions with  $\delta = 0$  for the  $E1$  primary and the secondary  $M1$  [4]  $\gamma$ -ray transition. Comparing both spin possibilities for the initial spin of the cascade, we notice that this cascade originates from a  $0^-$  capture state. A cascade that seems to originate mainly from a spin  $1^-$  capture state is shown in Fig. 3(b). We assumed a pure  $E1-E2$  cascade. In that case, the data points are not described as accurately as in the example given in Fig. 3(a). This might hint at a stronger mixing for this transition. Still it shows that the data can be explained rather by an  $E1-E2$  cascade from a  $1^-$  capture state than by an  $M2-E2$  cascade starting with a spin  $0^-$  initial state.

We presented the results of a  $\gamma\gamma$  angular-correlation experiment investigating  $^{200}\text{Hg}$  after cold-neutron capture at the ILL research reactor. Some of our determined multipole mixing ratios strongly differ from  $\delta$  values published in the recent data compilation [4]. The  $\delta$  values reported here impact theoretical interpretations of the nucleus, e.g., the discussion of mixed-symmetry states in Ref. [19], and should be considered in future. In addition, we investigated the nature of the neutron-capture state in  $^{200}\text{Hg}$  by analyzing its depopulating primary  $\gamma$  rays. In the literature [20,21] the neutron-capture state was published as spin  $0^-$ , but we could show a non-negligible spin  $1^-$  contribution.

We thank our co-workers at the IKP Cologne and the Nuclear and Particle Physics Group of the ILL for their collaboration, C. Dreschner from Universität Heidelberg for her support with setting up the experiment, and M. Elvers for his help with the Cologne Sorting Code. We also thank the PGAA group of FRM2 for providing the Teflon bag equipment for the target holders and the staff of the research reactor in Grenoble for the excellent beam conditions.

- 
- [1] K. S. Krane, *Introductory Nuclear Physics* (Wiley, New York, 1988).
  - [2] H. Häse *et al.*, *Nucl. Instrum. Methods Phys. Res., Sec. A* **485**, 453 (2002).
  - [3] H. Abele *et al.*, *Nucl. Instrum. Methods Phys. Res., Sec. A* **562**, 407 (2006).
  - [4] F. G. Kondev and S. Lalkovski, *Nucl. Data Sheets* **108**, 1471 (2007).
  - [5] B. Singh, *Nucl. Data Sheets* **108**, 79 (2007).
  - [6] M. A. Lone *et al.*, *Nucl. Phys. A* **243**, 413 (1975).
  - [7] W. Urban *et al.* (private communication).
  - [8] C. Bernards *et al.*, *Phys. Rev. C* **79**, 054307 (2009).
  - [9] C. Bernards *et al.*, *Phys. Rev. C* **81**, 024312 (2010).
  - [10] K. S. Krane *et al.*, *Nucl. Data Tables* **11**, 351 (1973).
  - [11] K. S. Krane and R. M. Steffen, *Phys. Rev. C* **2**, 724 (1970).
  - [12] W. D. Hamilton, *The Electromagnetic Interaction in Nuclear Spectroscopy* (North-Holland, Amsterdam, 1975).
  - [13] I. Wiedenhöver, code CORLEONE, University of Cologne, 1995.
  - [14] R. Casperson (private communication).
  - [15] H. J. Rose and D. M. Brink, *Rev. Mod. Phys.* **39**, 306 (1967).
  - [16] M. Sakai *et al.*, *Nucl. Phys.* **65**, 177 (1965).
  - [17] J. Hattula *et al.*, *Z. Phys.* **241**, 117 (1971).
  - [18] D. Breitig *et al.*, *Phys. Rev. C* **9**, 366 (1974).
  - [19] S. T. Ahmad *et al.*, *J. Phys. G* **15**, 93 (1989).
  - [20] R. E. Segel *et al.*, *Phys. Rev.* **133**, 7 (1964).
  - [21] L. M. Bollinger and R. E. Cote, *Bull. Am. Phys. Soc.* **5**, 294 (1960).
  - [22] R. F. Casten, *Nuclear Structure from a Simple Perspective* (Oxford University Press, New York, 1990).